CONNECTING THE WRONG DOTS: CAN THALAMO-CORTICAL DYSCONNECTIVITY EXPLAIN ALTERED COROLLARY DISCHARGE IN SCHIZOPHRENIA?

By

Beier Yao

A THESIS

Submitted to
Michigan State University
in partial fulfillment of the requirements
for the degree of

Psychology – Master of Arts

2018

ABSTRACT

CONNECTING THE WRONG DOTS: CAN THALAMO-CORTICAL DYSCONNECTIVITY EXPLAIN ALTERED COROLLARY DISCHARGE IN SCHIZOPHRENIA?

By

Beier Yao

Corollary discharge (CD) signals are "copies" of motor signals sent to sensory areas to predict the impending input. Because they are used to distinguish actions generated by oneself versus external forces, altered CD has been hypothesized to result in the commonly-observed agency disturbances in schizophrenia patients (SZP). Behavioral evidence for altered CD in SZP has been observed in multiple sensorimotor domains, including the oculomotor system; however, its exact neural underpinning is unknown. One oculomotor CD pathway identified in primates projects from motor neurons in the superior colliculus (SC) to visual neurons in the frontal eye fields (FEF) via the mediodorsal thalamus (MDT). The current study aimed to examine the structural connectivity of MDT-FEF pathway in SZP and whether it relates to oculomotor CD abnormalities. Twenty-four SZP and 22 healthy controls (HC) underwent diffusion tensor imaging (DTI), and a large subset of those individuals also performed the blanking task, an eye movement task that measures the influence of CD on visual perception. Probabilistic tractography was used to identify white matter tracts connecting FEF and MDT. Microstructural integrity of these tracts was compared across groups and correlated with behavioral indices of oculomotor CD from the blanking task and symptom severity. We found that SZP had compromised microstructural integrity in MDT-FEF pathway. This hypoconnectivity was correlated with both impaired oculomotor CD signals and more severe positive symptoms in SZP. These data suggest that the MDT-FEF pathway may serve an important role in transmitting oculomotor CD signals, which in turn may relate to positive symptom manifestation in SZP.

ACKNOWLEDGEMENTS

The author would like to thank Dr. Katy Thakkar for her guidance and support, Dr. Jason Moser and Dr. Mark Becker for their helpful feedback, Lara Rösler for sharing her analyses results, Jingtai Liu for his assistance on 3D tract visualization, Livon Ghermezi for visually inspecting part of the imaging data, Xiaochen Luo for providing constructive distractions and meaningful companionship, and all the participants for their participation.

TABLE OF CONTENTS

LIST OF TABLES

LIST OF FIGURES

INTRODUCTION

It has always been a challenge to come up with a mechanistic model of schizophrenia that explains its wide range of symptoms on both phenomenological and neurobiological levels. One recent theory that attempted to address this problem was the prediction error (PE) model of psychosis (Corlett, Honey, & Fletcher, 2016; Fletcher & Frith, 2009; Gray, Feldon, Rawlins, Hemsley, & Smith, 1991). Simply put, we form a model of the world that is based on sensory inputs and expectancies, and we update our model of the world whenever we encounter a PE – a mismatch between our prediction and actual sensory input, to make the model closer to the ever-changing reality. However, individuals with schizophrenia (SZP) may have excessive false PEs that constantly prompt them to update a perfectly working model. Because these abnormal PEs were due to systematically altered predictions rather than real changes in the environment, the model can never be updated satisfactorily, hence leading to unusual sensory experiences commonly seen in SZP.

To break the PE model down, basic predictions rely on simple correlations between commonly co-occurring stimulus-stimulus pairs (e.g. police cars by the roadside predict accidents) and action-stimulus pairs (e.g. speaking predicts hearing your own voice). This study focused on the latter. Predictions about our own actions are established via corollary discharge (CD), or efference copy, signals in our brains. CD signals are, in essence, "copies" of motor signals containing information about the intended movement (e.g. direction, amplitude, velocity, etc.). They originate from the same brain areas as the motor signals do but are then sent to sensory areas, where a prediction of the sensory consequences of the intended movement can be computed. This match between predicted and actual sensory inputs is argued to be the basis of our sense of agency - the subjective sense of being in control of the actions we produce.

However, an altered CD signal could lead directly to a wrong (or absent) prediction and hence a PE. One direct consequence then could be misattributing self-generated actions to external forces. Interestingly, almost all first rank symptoms of schizophrenia (Schneider, 1959)—symptoms which were argued to be pathognomonic to schizophrenia—could be conceptualized as agency disruptions, e.g. alien control delusions, auditory hallucinations (misattributing one's sub vocal voices as someone else speaking; Green & Kinsbourne, 1990). Therefore, altered CD has been theorized as the basis for these agency disruptions in schizophrenia (Feinberg, 1978). There is indeed a growing evidence base that CD is impaired in SZP in multiple sensory modalities (Blakemore, Smith, Steel, Johnstone, & Frith, 2000; Ford & Mathalon, 2012; Shergill, Samson, Bays, Frith, & Wolpert, 2005). A thorough understanding of how CD signals go awry in the brains of SZPs can shed light on key mechanisms of the disorder and help develop more targeted interventions.

One potential neural pathway transmitting CD signals associated with saccadic eye movements has been identified in recent primate studies: neurons in the mediodorsal thalamus (MDT) seem to play a crucial role in relaying CD signals originating from movement neurons in the superior colliculus (SC) to the visual neurons in the frontal eye fields (FEF; Sommer & Wurtz, 2002, 2004, 2008). Results from humans with specific MDT lesions support this finding (Gaymard, Rivaud, & Pierrot-Deseilligny, 1994; Ostendorf, Liebermann, & Ploner, 2010). A large body of animal physiology work supports the notion that the thalamus may play a more general key role in transmitting CD signals. The branching axons innervating thalamus enable the distribution of an identical message to both motor centers and sensory areas, making them a strong candidate for CD circuits that permit sensory predictions of almost all motor actions (Sherman, 2016). If this is the case, then thalamus essentially helps modulate all cortical

processing of motor commands. In other words, thalamo-cortical connectivity could play a crucial role in abnormal transmission of CD signals. Interestingly, there has long been a model of schizophrenia as a "misconnection syndrome", in which thalamus is a key link (Andreasen, 1999). Altered CD could be a direct consequence of misconnection in neural circuits and could be a more proximal mechanism of schizophrenia symptoms. Though there is mounting behavioral evidence for altered oculomotor CD in SZP (See Thakkar, Diwadkar, & Rolfs, 2017 for review), no study to date has studied whether abnormalities in the MDT-FEF pathway contribute to this.

Corollary discharge abnormalities in psychosis

To date, most of our understanding of CD in human and non-human primates comes from the oculomotor system. Current evidence indicates that we rely on CD signals for different oculomotor processes such as maintaining visual stability (i.e. perceiving a stable and continuous world despite constant eye movements; Cavanagh, Hunt, Afraz, & Rolfs, 2010) and generating rapid successive goal-directed saccades (i.e. preparing a second saccade command while executing the first saccade; Hallett & Lightstone, 1976a, 1976b). Likewise, a large body of evidence for CD abnormalities in psychosis also comes from the oculomotor system (see Thakkar et al., 2017 for review).

One commonly used task to assess visual stability is the blanking task, which measures visual perception shortly following an eye movement (Figure 1; Deubel, Schneider, & Bridgeman, 1996). In this task, following a period of fixation, a visual stimulus appears at a peripheral location on the screen (at the *pre-saccadic location*), and the participant is instructed to look at the stimulus. Once the participant initiates a saccade, the stimulus disappears for a brief moment and reappears at a new location (*post-saccadic location*) slightly backward or

forward relative to the pre-saccadic location. The participant is then asked to judge in which direction the stimulus jumped relative to its pre-saccadic location. Because saccadic eye movements are often imprecise, the saccade typically falls short or long of the target. Therefore, the participant cannot rely on the saccade landing site to inform them of the pre-saccadic location to make an accurate judgment on the post-saccadic location. For example, if the stimulus jumps backward by 0.5° and the saccade falls short of the target by 1° (i.e. 0.5° short of the post-saccadic location), it will appear that the stimulus jumps *forward* relative to the *saccade landing site* (see Figure 2 for an illustration). The participant has to "know" by exactly how much the saccade fell short or long of target in order to remap the actual pre-saccadic location correctly, which requires access to information stored in a CD signal. In other words, if CD signals are intact, there should be no correlation between the actual saccade landing site and the participant's perceptual judgment –saccades falling short or long of the target are random errors that have no relationship with the pre-saccadic location, and hence should have no influence on the judgment of post-saccadic location either. Indeed, this is exactly how healthy people perform on the task (Collins, Rolfs, Deubel, & Cavanagh, 2009). However, if CD signals are compromised, the participant may not have access to enough information about the spatial accuracy of the saccade. In such a case, the participant can only rely on the actual saccade landing site to make the perceptual judgment - there is no information that would prompt the participant to think that the saccade was not precise. Therefore, when CD is impaired, one would expect to see a correlation between the saccade landing site and the participant's perceptual judgment because as the saccade falls increasingly short of the target, there is a greater chance that the post-saccadic location will be forward of the saccade landing site. This has indeed been observed in humans with MDT lesions (Ostendorf et al., 2010) and in primates whose MDT was

temporarily inactivated (Cavanaugh, Berman, Joiner, & Wurtz, 2016), providing more evidence to suggest that MDT is a key relay station for CD signals related to saccadic eye movements.

Recently, Rösler and colleagues (2015) examined CD in SZP using the blanking task. SZP exhibited reduced precision of perceptual judgments, as evidenced by flatter psychometric curves plotting performance against target displacement. That is, their perceptual judgments were less sensitive to the actual target displacement. On a group level, they found a correlation between saccade landing site and perceptual judgment in SZP, but not in HC (Figure 3), consistent with previous literature of impaired oculomotor CD in SZP. That is, SZP with shorter mean saccade amplitudes made more forward judgements. Although this relationship did not manifest on the single-subject level for most participants, SZP with more severe positive symptoms showed a greater reliance on saccade landing sites (Figure 4), supporting the theory that abnormal CD is a key mechanism of psychosis (Feinberg & Guazzelli, 1999).

Altered thalamo-cortical connectivity in schizophrenia

There is growing evidence that thalamo-cortical connectivity is impaired in schizophrenia and is closely related to symptomatology and functioning. Recent structural imaging studies found white matter alterations in thalamo-cortical circuits across different illness stages (see Canu, Agosta, & Filippi, 2015 for review), which are consistent with altered functional connectivity in thalamo-cortical circuits (see Pergola, Selvaggi, Trizio, Bertolino, & Blasi, 2015 for review). More specifically, pathways involving MDT and its projection sites in frontal cortex seem to have the strongest support for being crucial to the pathophysiology of schizophrenia, though not many studies have examined individual thalamic nuclei (Anticevic, Cole, et al., 2014; Giraldo-Chica, Rogers, Damon, Landman, & Woodward, 2018; Shepherd, Laurens, Matheson, Carr, & Green, 2012; Woodward, Karbasforoushan, & Heckers, 2012). Importantly, thalamo-

frontal hypoconnectivity has also been found in individuals at clinical high risk for psychosis and bipolar patients with a history of psychosis (Anticevic et al., 2015; Anticevic, Yang, et al., 2014), ruling out medication effects or illness chronicity as main contributors and suggesting that thalamo-frontal hypoconnectivity may relate to psychosis in a trans-diagnostic manner. Attesting to their clinical relevance, these white matter alterations are further correlated with clinical symptoms, cognitive impairments, and treatment outcomes (see Canu et al., 2015 for review). Relevant to this study, there is evidence that SZP with passivity symptoms (i.e. symptoms related to a sense of losing agency over one's body/thoughts, directly reflecting altered CD) have more compromised white matter integrity in thalamus, relative to SZP without passivity symptoms (Sim et al., 2009). This provides indirect evidence for our hypothesis that impaired thalamo-cortical structural connectivity may underlie the CD abnormalities in schizophrenia, which we propose could be a key mechanism of symptom expression of the disease.

In this study, we used diffusion tensor imaging (DTI) and the blanking task to study white matter connectivity and oculomotor CD in SZP, respectively. DTI is an imaging method commonly used to assess structural connectivity in human brains. Specifically, we tested the following three hypotheses: (1) there will be abnormal structural connectivity in the MDT-FEF pathway in SZP relative to HC; (2) connectivity of the MDT-FEF pathway will be positively correlated with oculomotor indices of CD signal integrity; (3) the integrity of MDT-FEF white matter pathway will also be correlated inversely with positive symptom severity in SZP.

METHODS

Overview

Participants performed the blanking task and underwent DTI. Putative white matter tracts connecting our regions of interest (ROIs) were computed using probabilistic tractography, an analysis technique that reconstructs anatomical pathways (presumably white matter tracts) between any given brain regions based on a distribution profile of probable fiber orientations in each voxel (Behrens et al., 2003; Behrens, Berg, Jbabdi, Rushworth, & Woolrich, 2007). The FEF was defined based on group-level functional MRI (fMRI) activation maps from the same subjects performing a different saccadic eye movement task in the scanner (Thakkar, van den Heiligenberg, Kahn, & Neggers, 2014). The MDT was localized using the Harvard-Oxford thalamic connectivity atlas, a probabilistic atlas of 7 sub-thalamic regions segmented according to their white matter connectivity to cortical areas (Desikan et al., 2006). Participants' individual probabilistic tracts in native space were normalized into a common space and averaged within groups. Then a threshold was applied to obtain final group tracts. Within each group-averaged tract, mean fractional anisotropy (FA), mean diffusivity (MD), axial diffusivity (AD), and radial diffusivity (RD) were then calculated for each participant. These indices of microstructural integrity of white matter tracts were used for further group comparisons and correlation analyses with behavioral indices of CD obtained from the blanking task, as well as symptom scores within the patient group.

Participants

Twenty-two antipsychotic-medicated SZP were recruited from a longitudinal study (Genetic Risk and Outcome in Psychosis (GROUP) Investigators, 2011) and an outpatient psychiatric facility in The Netherlands. Schizophrenia or schizoaffective disorder diagnoses were based on

Diagnostic and Statistical Manual of Mental Disorders, fourth edition (DSM-IV) criteria and verified with the Comprehensive Assessment of Symptoms and History interview (Andreasen, Flaum, & Arndt, 1992) or Schedules for Clinical Assessment for Neuropsychiatry, version 2.1 (Wing et al., 1990). Chlorpromazine (CPZ) equivalent antipsychotic dosages were calculated for each patient (Woods, 2003). Clinical symptoms were assessed with the Positive and Negative Syndrome Scale (PANSS; Kay, Fiszbein, & Opler, 1987). Twenty-four HC without a personal or family history of DSM-IV Axis I diagnosis were recruited via community advertisements. Criteria for participant exclusion were a history of head trauma or neurological illness and recent substance abuse or dependence. All subjects gave written informed consent and were reimbursed for participation. The study was approved by the Human Ethics Committee of the University Medical Center, Utrecht.

Blanking task

This task measures the degree to which CD influences visual perception immediately following a saccade (Figure 1). Each trial started with the participant fixating on a red circle on a grey background in a dimly lit room. To reduce anticipation effect or stereotypical behavior (Collins et al., 2009), the circle randomly appeared at one of six locations (a combination of a 1° or −1° of visual angle displacement horizontally and a 0°, 1°, or −1° displacement vertically relative to the center of the screen) with equal probability. Once the eye tracker detected that the participant had maintained fixation for 200 ms, the circle would turn black. After a random delay of 500-1000 ms, the circle reappeared at a new location 10° to the left or right of the fixation position (*pre-saccadic location*). The participant was instructed to look at the stimulus as quickly as possible. Once the participant initiated a saccade, the stimulus would disappear (i.e. blank) for 250 ms and reappear at a location (*post-saccadic location*) somewhere between −3° to 3° (in

increments of 0.5°) to the left or right of the pre-saccadic location and would stay on the screen for the remainder of the trial. The participant was then asked to report in which direction the stimulus jumped relative to its pre-saccadic location by key pressing. Although participants indicated a left or right response, for analysis purposes we recoded these responses: "forward" means jumping away from the fixation position, and "backward" means jumping towards the fixation. The combination of 6 fixation positions × 13 post-saccadic locations (including 0° displacement) × 2 directions (left, right) resulted in 156 total trials. Duration of the task varied across participants and typically ranged from 15 to 30 minutes. See Rösler et al., 2015 for more details on the eye-tracking apparatus and task stimuli. Eighteen SZP and 17 HC reported in Rösler et al., 2015 also participated in this study and their data was used in the analyses involving blanking task performance.

Participants' performance on this paradigm was already analyzed and reported elsewhere (Rösler et al., 2015). For this study, two measures of CD were used in relevant statistical analyses: just noticeable difference (JND) and the loss slope. Briefly, for each individual, trials were collapsed across fixation positions and saccade directions. A logistic function was fit to the data plotting percentage of forward responses as a function of target displacement (i.e. the position of post-saccadic location relative to the pre-saccadic location; see Figure 5 for examples). A **JND** was derived from the function as the difference in target displacements between the points where the function reached 50% and 75% of its full growth. This measure indicates individuals' sensitivity to target displacement, which presumably relies on CD input to infer the pre-saccadic location. Therefore, smaller JND indicates greater CD integrity. Next, for each individual, trials were collapsed across target displacements. Landing site errors (i.e. distance between the actual saccade landing site and the pre-saccadic location) were divided into

multiple bins. Mean saccade landing site was then calculated for each bin. The **loss slope** was derived from a weighted linear regression where percentage of forward responses corresponding to each bin was fit against mean saccade landing site per bin, weighted by the number of trials per bin. Because individuals with intact CD signals should not rely on saccade landing sites to make perceptual judgments about target displacements, the slope should be almost zero in HC. More negative slope values indicate more reliance on landing site and therefore a larger loss of CD signals, hence the name "loss slope."

Image acquisition

All DTI data were acquired at the University Medical Center Utrecht on a Philips Achieva 3T scanner (Philips Medical Systems, Best, The Netherlands) equipped with an eight-channel head coil allowing parallel imaging. Two diffusion images were acquired using single-shot echoplanar imaging sequences, consisting of 30 diffusion-weighted scans (b = 1,000 s/mm^2) with noncollinear gradient directions and one image without diffusion weighting (b = 0 s/ mm^2), covering the entire brain (Repetition Time (TR) = 7,057 ms; Echo Time (TE) = 68 ms; field of view = 240 mm × 240 mm × 150 mm; in plane resolution = 1.875 mm × 1.875 mm; slice thickness = 2 mm; no slice gap; 75 axial slices; matrix size 128 mm × 99 mm). The diffusion weighted scans were measured twice, once with phase encoding direction reversed (first scan posterior-anterior, second scan anterior-posterior), in order to correct for susceptibility induced spatial distortions (Andersson & Skare, 2002). For registration purposes, a whole-brain three-dimensional T1-weighted scan (200 slices; TR = 10 ms; TE = 4.6 ms; flip angle = 8°; field of view, 240 mm × 240 mm × 160 mm; voxel size: 0.75 mm × 0.8mm × 0.75 mm) was acquired.

Regions of interest

We included two regions of interest (ROIs) in each hemisphere: FEF and MDT. As FEF does not have clear anatomical boundaries, the group-level functional MRI (fMRI) activation maps from the same subjects performing a different saccadic eye movement task in the scanner (Thakkar et al., 2014) were used to define this region. More specifically, FEF was created based on areas that showed greater activation on trials during which participants were making saccades versus where they were fixating (threshold $p < 0.001$ uncorrected) across both groups. The thalamus was localized using the Harvard-Oxford thalamic connectivity atlas, which is a probabilistic atlas of 7 sub-thalamic regions segmented according to their white matter connectivity to cortical areas (Desikan et al., 2006). MDT was operationally defined as the region of the atlas with highest probability ($\geq 25\%$) of connectivity to the prefrontal cortex. Both ROIs were limited to white matter structure only and did not include grey matter. Individual white matter masks were created by first segmenting the T1 image into grey matter, white matter, and cerebrospinal fluid using SPM, and then extracting those voxels that had the highest probability of being identified as white matter.

Preprocessing

The diffusion-weighted scans were preprocessed and analyzed using FSL 5.0 (FMRIB's Software Library, www.fmrib.ox.ac.uk/fsl). As DTI scans suffer from spatial distortions along the phase encoding direction, two diffusion-weighted scans were acquired with reversed phase encoding blips, resulting in pairs of images with distortions going in opposite directions. From these two images, the off-resonance field were estimated using a method similar to that described by Andersson and Skare (2002) as implemented in FSL (Smith et al., 2004). Next, the 30 diffusion-weighted images from each phase-encoding direction were realigned to the b0 image

using affine registration, and eddy current correction was applied. The eddy-corrected scans with opposite phase encoding blips were then combined into a single corrected image using the previously estimated off-resonance field. A brain mask was created for the mean b0 image and applied to all diffusion-weighted images. DTI analyses must be performed in native space as diffusion gradients are specified in this space; however, ROIs were created in standard (Montreal neuroimaging; MNI) space. To transform the ROIs into each subject's native space, the anatomical T1-weighted volume was realigned to the mean b0-weighted image and subsequently normalized to MNI-space using the unified segmentation algorithm as implemented in SPM8 (Ashburner & Friston, 2005). The inverse warping parameters from this step were used to transform ROIs from MNI space to native space (Neggers, Zandbelt, Schall, & Schall, 2015).

Probabilistic tractography

We performed probabilistic tractography between MDT and FEF in both hemispheres from both directions (i.e. MDT to FEF and FEF to MDT), each serving as both a seed (start point) and a target (end point), since diffusion MRI cannot distinguish between forward and backward projections. The distribution profile of probabilistic connectivity is computed by iteratively sending out 5000 streamlines from the seed area, going through all probable principal diffusion directions in each voxel until it was determined impossible to continue. Only streamlines that reached the target successfully were included in the analysis, and streamlines were not allowed to continue after reaching the target. Two crossing fibers per voxel were allowed. In addition, the mid-sagittal plane was used as exclusion mask to avoid streamlines travelling falsely into the other hemisphere (Landman et al., 2012; Mori & van Zijl, 2002; Mori & Zhang, 2006). Upon examination of preliminary tractography results, an axial plane located one voxel beneath MDT

was added as another exclusion mask to avoid streamlines travelling in the opposite direction of FEF and looping back on themselves.

For each subject, a "connectivity value" was generated for each voxel at the end of the tractography process by computing the number of streamlines going through the specific voxel. Therefore, higher values indicate a higher probability that the voxel belongs to the tract of interest. In order to perform group analyses, individual tractography results were transformed to MNI space. To make sure only white matter structures were included in the analyses, each individual's whole brain white matter map was used as a mask to preserve connectivity values in these structures only. After that, these values were averaged across participants within each group.

Connectivity values are not only determined by actual structural connectivity, but also influenced by other factors like size of the seed ROI (i.e. bigger seeds send out more streamlines). Thus, higher connectivity values in a given tract do not necessarily indicate a larger probability of an actual structural connection. That is, the number of streamlines passing through a given voxel cannot be directly compared across seed/target combinations. Therefore, to avoid potential biases, we did not use the same absolute value for thresholding each group-averaged tract but used the top 0.27% (3σ above mean in normal distribution) of all voxels as the threshold instead. After applying the threshold, these group tracts were binarized into masks per tract. Masks from both directions (i.e. FEF to MDT and MDT to FEF) were considered equally accurate and combined to achieve a single mask for the MDT-FEF pathway per each group.

For each participant, mean FA, MD, AD, and RD within each of the group-thresholded tracts were extracted. FA is currently the most widely used measure of anisotropy, highly sensitive to microstructural integrity of white matter tracts. Higher FA value means higher anisotropy and

lower diffusivity (e.g. better microstructural integrity). However, FA value contains no information on the orientation of anisotropy and thus can be difficult to interpret in isolation. A decrease in FA could be caused by multiple factors: white matter neuropathology, fiber crossing, normal aging, etc. (Alexander, Lee, Lazar, & Field, 2007). Therefore, it is recommended to use multiple measures for better understanding of the microstructure of white matter. Specifically, RD appears to be a more sensitive indicator of myelination, while AD seems to indicate axonal degeneration (Song et al., 2002). MD seems to be best at assessing white matter maturation and aging (Abe et al., 2002; Snook, Plewes, & Beaulieu, 2007). Higher values for RD, AD, and MD mean higher diffusivity (e.g. poorer microstructural integrity).

Statistical analyses

Statistical analyses were performed using IBM SPSS Statistics 20.0 (IBM, Armonk, NY). First, to examine group differences of tract locations, a probability value was calculated for each voxel by dividing the number of tracts going through the voxel by the total number of tracts in the MDT-FEF pathway in each hemisphere. This value indicates the probability of the specific voxel belonging to the actual MDT-FEF structural connection. Then between-group t-tests were performed on probability values at each voxel on the whole brain level with family-wise error correction using SPM. Next, to compare microstructural integrity of MDT-FEF white matter tracts, repeated measures ANOVAs were conducted on each of the four microstructural integrity measures (FA, MD, RD, and AD), including diagnostic group as a between-subjects variable and hemisphere as a within-subject variable.

Since we were interested in the specific influence of structural connections between MDT and FEF on behavior, mean integrity measures over the whole brain were regressed out of the tract measures that did not differ between hemispheres. For measures with a significant

hemisphere effect or hemisphere by group interaction, mean integrity measures over each hemisphere were regressed out of the corresponding tract measures. These standardized residuals were used for all the correlation analyses. All standardized values are 0 when equal to the whole brain average of the corresponding measure. For standardized residuals of FA, higher values indicate more anisotropic voxels and lower more isotropic voxels (i.e. more impaired integrity). For standardized residuals of MD, RD, and AD, higher values indicate more diffusive voxels, and lower values less diffusive. We performed Pearson correlation analyses between two behavioral measures (loss slope and JND) and the standardized residuals. Using SZP data only, we conducted Spearman's rank correlation analyses between PANSS subscale scores (positive and negative symptoms) and standardized residuals. To examine potential confounding effects of antipsychotic use, standardized medication dose was correlated with the behavioral measures and the microstructural integrity measures.

RESULTS

Participant characteristics

The SZP and HC were matched for sex, age, IQ, and handedness. See Table 1 for detailed participant characteristics. Only a subset of the sample (18 SZP, 17 HC) has both DTI and behavioral data. The two groups in this subset also did not differ on sex, age, IQ, and handedness (Table S1).

Hypoconnectivity in MDT-FEF pathway

The spatially normalized, group-averaged, and statistically thresholded MDT-FEF probabilistic tracts in both the left and right hemisphere are shown in Figure 6 and Figure 7. We performed a between-group t-test on whole brain probability values at each voxel. No significant differences were found between the SZP and HC at the family-wise error rate of 0.05, indicating that the MDT-FEF pathway occupied the same spatial location in the brain.

Next, we conducted four repeated measures ANOVAs where one of the microstructural integrity measures (FA, MD, RD, AD) was the dependent variable each time, using diagnostic group as a between-subjects variable and hemisphere as a within-subject variable (see Figure 8). Means and standard deviations are presented in Table 2. Again, higher microstructural integrity is indicated by higher FA values and lower MD, RD, and AD values. For FA, MD, and RD, there was a significant effect of group such that SZP showed evidence of reduced microstructural integrity of the MDT-FEF pathway (FA: $F(1,44) = 11.05$, $p = 0.002$, partial $\eta^2 = 0.20$; MD: $F(1,44) = 4.69$, $p = 0.036$, partial $\eta^2 = 0.10$; RD: $F(1,44) = 10.88$, $p = 0.002$, partial $\eta^2 = 0.20$). There was no group difference in tract AD, $F(1,44) = 0.001$, $p = 0.98$, partial $\eta^2 = 0.00$. For FA and RD, there was an additional group × hemisphere interaction effect (FA: $F(1, 44) = 31.98$, $p < 0.001$, partial $\eta^2 = 0.42$; RD: $F(1, 44) = 13.16$, $p = 0.001$, partial $\eta^2 = 0.23$), such that these

measures only differed significantly between groups in the right hemisphere (FA: $t(44) = 5.86$, $p < 0.001$; RD: $t(44) = 4.63$, $p < 0.001$; Table 2). This group × hemisphere interaction effect was not significant for MD, $F(1,44) = 0.42$, $p = 0.52$, partial $\eta^2 = 0.01$. Finally, there was no main effect of hemisphere for any of the measures. There were no correlations between CPZ equivalent dose and any of the microstructural integrity measures ($-0.44 < r_s < 0.25$, $0.07 < p < 0.98$). In the subsample of participants with behavioral data, there was still a main effect of group on FA, MD, and RD, such that patients showed reduced microstructural integrity. Complete results from this subsample are presented in Supplementary Results.

Relationship with oculomotor CD

Because we only found significant group differences in FA, MD, and RD, we performed Pearson correlation analyses between the standardized residuals of these three measures (after controlling for variance due to whole brain structural integrity) and two behavioral measures (loss slope and JND). In SZP only, we found a significant correlation between standardized residual of MD and JND ($r = 0.57$, $p = 0.013$) and a significant correlation between standardized residual of RD in the left tract and JND ($r = 0.47$, $p = 0.049$; see Figure 9). Combined, these results are consistent with our predictions: higher JND, which is indicative of poorer CD signaling, is related to compromised white matter integrity in the MDT-FEF pathway in SZP. No correlations were found between the loss slope and the standardized residuals. No correlations were found between the blanking task measures and standardized residuals in HC. There were no correlations between CPZ equivalent dose and the behavioral measures in SZP (JND: $r_s = -0.31$, $p = 0.24$; loss slope: $r_s = 0.42$, $p = 0.11$).

Relationship with clinical symptoms

Lastly, we conducted Spearman's rank correlation analyses between PANSS subscale scores (positive and negative symptoms) and the three residual tract measures (FA, MD, RD) that were altered in SZP. We found a significant correlation between MD residual values and PANSS positive symptom score ($r_s = 0.43$, $p = 0.047$) and between standardized residual of RD in the left tract and PANSS positive symptom score ($r_s = 0.48$, $p = 0.026$; see Figure 10). No correlations were found between PANSS negative symptom score and the standardized residuals (MD: $r_s = 0.12$, $p = 0.58$; left RD: $r_s = 0.08$, $p = 0.74$). Taken together, these correlations suggest that more severe positive symptoms in SZP, but not negative symptoms, were associated with compromised white matter integrity in the MDT-FEF pathway.

DISCUSSION

In this study, we examined whether SZP differed from HC on the microstructural integrity of the MDT-FEF pathway, and whether putative abnormalities were correlated with behavioral indices of oculomotor CD and psychotic symptoms. Using DTI and probabilistic tractography, we found that SZP and HC shared the same spatial location of the tracts connecting MDT and FEF. However, SZP had compromised microstructural integrity of these tracts, such that they had lower FA and higher MD and RD than HC. This hypoconnectivity was found to further correlate with behavioral indices of reduced oculomotor CD signaling and more severe positive symptoms in SZP, indicating a potential disease mechanism that has specific behavioral correlates and symptom implications.

Our finding that SZP had reduced MDT-FEF structural connectivity is consistent with recent findings of white matter alterations in prefrontal-thalamic pathways in SZP (Canu et al., 2015; Giraldo-Chica et al., 2018). This was also consistent with previous functional connectivity findings of reduced prefrontal-MDT connectivity in SZP (Anticevic, Cole, et al., 2014; Welsh, Chen, & Taylor, 2010; Woodward et al., 2012) and thalamo-prefrontal hypoconnectivity in clinical high risk populations (Anticevic et al., 2015). Notably, there have been consistent case reports on patients with MDT lesions experiencing psychotic-like symptoms such as hallucinations and delusions (Carrera & Bogousslavsky, 2006; Crail-Melendez, Atriano-Mendieta, Carrillo-Meza, & Ramirez-Bermudez, 2013; Zhou et al., 2015), supporting the link between thalamo-cortical communication and positive symptom formation.

Besides decreased FA, SZP also exhibited increased MD and RD in the MDT-FEF pathway in current study. As a marker of normal aging (Abe et al., 2002), our finding of increased MD in SZP provides indirect evidence supporting the accelerated aging theory of

schizophrenia (see Islam, Mulsant, Voineskos, & Rajji, 2017 for review). In fact, a recent study found that the rate of white matter decline was 60% steeper in SZP than in HC and the difference was present throughout the life span (Cropley et al., 2017). On the neurobiological level, increased RD in SZP indicated that the hypoconnectivity might be related to myelin and oligodendroglia dysfunctions (Davis et al., 2003).

Somewhat surprisingly, we also found a significant group by hemisphere interaction effect in FA and RD. To date, very few studies have assessed the connectivity between specific thalamic nuclei and cortical areas in SZP. In the few studies that examined MDT-cortical functional connectivity, a group by hemisphere interaction was either not modeled, not reported, or not found (Anticevic, Cole, et al., 2014; Welsh et al., 2010; Woodward et al., 2012). One recent structural imaging study that found decreased prefrontal-MDT connectivity in SZP reported a more prominent difference in the left hemisphere (Giraldo-Chica et al., 2018), contrary to our finding of a more prominent difference in the right hemisphere. However, there were a few key differences between their study and the current one. First, the SZP group in their study was approximately 10 years younger and was earlier in the course of illness. Second, and perhaps more importantly, their main connectivity analyses used "total connectivity" values (calculated by dividing the number of streamlines reaching a certain cortical area by the number of streamlines reaching all cortical regions from thalamus), rather than indices of microstructural integrity such as FA and MD. In other words, their group comparison revealed the differences in whole brain thalamo-cortical connectivity patterns (i.e. how thalamo-cortical connectivity was distributed among different cortical regions), rather than the absolute difference on microstructural level within a specific thalamo-cortical pathway such as prefrontal-thalamic

connection. Clearly, more research is needed to address whether there is a hemispheric effect to the altered thalamo-prefrontal connectivity, or thalamo-cortical connectivity in general, in SZP.

The most novel and arguably most important finding of current study is that we found a relationship between the MDT-FEF structural connectivity and oculomotor CD signal integrity, mirroring findings from primate neurophysiology studies (Sommer & Wurtz, 2008). In other words, one interpretation of the current findings is that due to reduced connectivity between MDT and FEF, oculomotor CD signals may have been lost or disrupted, resulting in poorer behavioral performance on the blanking task. Presumably, the other consequence of these compromised CD signals were frequent inaccurate predictions about visual inputs, which then led to constant false PEs that were ultimately "resolved" by abnormal perceptual experiences. This could potentially explain the correlation between the MDT-FEF hypoconnectivity and positive symptom severity and the lack of correlation with negative symptom severity. Because whole brain white matter connectivity differences were already regressed out in the correlation analyses, this relationship between white matter integrity and positive symptom was specific to the MDT-FEF pathway rather than a result of general reduced structural connectivity. Taken together, the MDT-FEF white matter tracts seem to play a key role in transmitting oculomotor CD signals that may also explain some of the symptom manifestation in SZP. This highlights the importance of thalamo-cortical connectivity as a potential biomarker of and/or a treatment target for schizophrenia (Ramsay & MacDonald, 2018).

The interpretation of current findings is limited by several factors. First, JND may not be the best indicator of CD signaling in the blanking task because it is also affected by general sources of noise (e.g. in visual input or in effector output). Indeed, it has been found that SZP have a wide range of visual processing deficits (reviewed in Yoon, Sheremata, Rokem, & Silver,

2013). A more sensitive index of CD signaling would be the loss slope obtained from the blanking task. However, we did not find any correlations between the loss slope and the microstructural integrity indices. One potential explanation is that SZP may fail to encode the pre-saccadic target locations properly due to impaired spatial working memory (Lee & Park, 2005), resulting in noisier perceptual judgments on the single-trial level. Consequently, due to a relatively small trial number, the regression analyses may not be powerful enough to obtain the most accurate estimates of loss slopes. Future studies utilizing more trials may help resolve this issue. Second, we would expect that altered CD should most directly relate to symptoms explained by agency loss; however, we did not include measures that assessed agency disturbances directly. Future studies should employ a more comprehensive and detailed measure on agency disruptions to test a more fine-grained hypothesis of the role that the MDT-FEF pathway plays in the PE model of psychosis. Nevertheless, altered CD has been posited as a general mechanism underlying hallucinations and delusions (Corlett et al., 2016), which were both captured by the PANSS positive symptom score. Third, SZP in the current study were relatively high-functioning and exhibited a limited range of symptom severity. Future studies using a more clinically heterogeneous sample (e.g. recent-onset and unmedicated patients) could further inform the relationships between thalamo-cortical structural connectivity and clinical status in SZP. Lastly, we were not able to rule out potential confounding effects of antipsychotic treatment because current study used a medicated sample. However, the CPZ equivalent dose did not correlate with any of the behavioral or microstructural measures.

We anticipate that findings from current study will pave the way for more in-depth mechanistic questions on CD and psychosis. In terms of future directions, studies utilizing larger sample size are necessary to obtain adequate power for regression analyses in which white matter

connectivity indices, behavioral indices of oculomotor CD, and symptom severity could be entered into one model, allowing us to test the hypothesis that structural connectivity in the MDT-FEF pathway directly mediates the relationship between oculomotor CD signaling abnormalities and positive symptom severity. Second, to better inform treatment development, a causal or directional relationship between white matter integrity, oculomotor CD signals, and psychotic symptoms is necessary. Future studies could try to establish directions in the brain-behavior correlations observed in current study by following clinical high risk populations over time and measuring their white matter integrity and behavioral indices of CD signaling before and after the onset of illness. Third, it is important to know whether altered CD is a phenotype of psychosis in general or a specific biomarker of schizophrenia spectrum disorders. To this date, only one study has found that CD in the auditory domain was similarly impaired in SZP and bipolar patients with a history of psychotic features (Ford et al., 2013). More replications in recent-onset affective and non-affective psychotic disorders, clinical high risk populations, and unaffected first-degree relatives are needed to address this question. The presence of altered CD in healthy relatives would provide evidence that CD abnormalities represent vulnerability towards psychosis, but that other factors are involved in the expression of full-blown psychosis.

In conclusion, we identified significant decreases in white matter connectivity in SZP relative to HC in the MDT-FEF pathway, which belongs to a key neural circuit transmitting oculomotor CD signals previously established in the animal literature. We demonstrated that hypoconnectivity in the MDT-FEF pathway was correlated with impaired oculomotor CD signals and more severe positive symptoms in SZP. These findings have important disease mechanism and treatment implications.

APPENDICES

APPENDIX A: Tables

Table 1. Demographic information.

	HC (n = 24)	SZP (n = 22)		
	Mean (SD)	Mean (SD)	Statistic	p
Age (Years)	34.9 (8.1)	37.4 (7.8)	t = -1.1	0.29
Sex (Female/Male)	11/13	5/17	χ^2 = 2.7	0.13
IQ[a]	100.4 (13.8)	96.0 (12.8)	t = 1.1	0.29
Education[b]	7.2 (1.3)	4.8 (1.7)	t = 5.2	< .001
Handedness[c]	0.89 (0.41)	0.85 (0.45)	t = 0.35	0.73
Illness Duration (Years)		14.2 (5.2)		
PANSS Positive		11.6 (5.2)		
PANSS Negative		13.1 (6.3)		
PANSS General		25.0 (7.9)		
CPZ Equivalent (mg)		281.3 (249.6)		

Notes: CPZ, chlorpromazine; HC, healthy control subjects; PANSS, Positive and Negative Syndrome Scale; SZP, patients with schizophrenia.
[a]Based on the Nederlandse Leestest voor Volwassenen.
[b]Education category: 0 = <6 years of primary education; 1 = finished 6 years of primary education; 2 = 6 years of primary education and low-level secondary education; 3 = 4 years of low-level secondary education; 4 = 4 years of average-level secondary education; 5 = 5 years of average-level secondary education; 6 = 4 years of secondary vocational training; 7 = 4 years of high-level professional education; 8 = university degree.
[c]Based on the Edinburgh Handedness Inventory; scores range from 0 indicating complete left-handedness to 1 indicating complete right-handedness.

Table 2. Mean microstructural integrity measures (FA, MD, RD, AD) in the MDT-FEF tract by hemisphere.

		HC (n = 24)	SZP (n = 22)
		Mean (SD)	Mean (SD)
FA	Left	0.41 (0.02)	0.41 (0.02)
	Right	0.42 (0.02)	0.39 (0.02)
MD	Left	7.05×10^{-4} (2.40×10^{-5})	7.18×10^{-4} (2.65×10^{-5})
	Right	7.06×10^{-4} (1.84×10^{-5})	7.21×10^{-4} (2.51×10^{-5})
RD	Left	5.43×10^{-4} (2.57×10^{-5})	5.56×10^{-4} (2.46×10^{-5})
	Right	5.36×10^{-4} (1.82×10^{-5})	5.66×10^{-4} (2.59×10^{-5})
AD	Left	1.03×10^{-3} (3.72×10^{-5})	1.04×10^{-3} (3.70×10^{-5})
	Right	1.05×10^{-3} (3.12×10^{-5})	1.03×10^{-3} (2.92×10^{-5})

Notes: AD: axial diffusivity; FA, fractional anisotropy; FEF, frontal eye fields; HC, healthy controls; MD, mean diffusivity; MDT, mediodorsal thalamus; RD, radial diffusivity; SZP, schizophrenia patients.

APPENDIX B: Figures

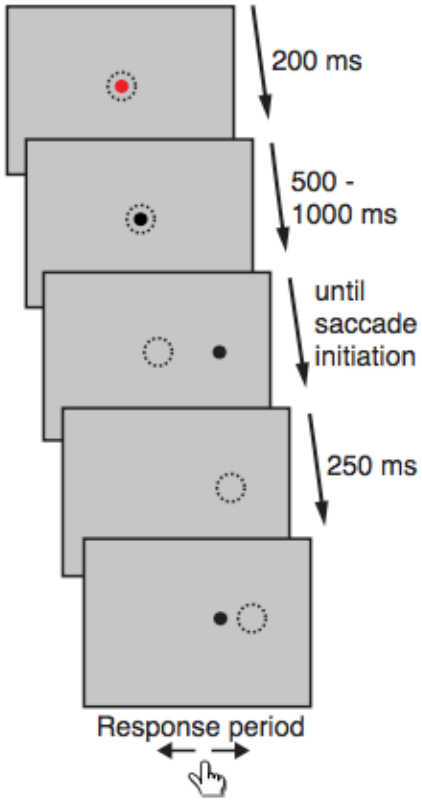

Figure 1. Blanking task. Dotted circles represent gaze positions (Rösler et al., 2015).

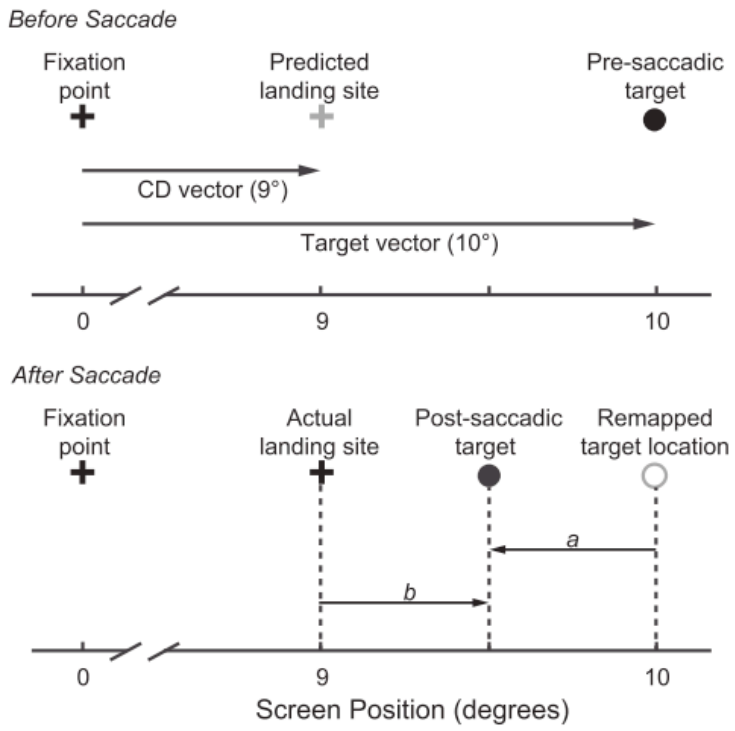

Figure 2. Blanking task perceptual judgment. Top: After the stimulus appears at the pre-saccadic location, a corollary discharge (CD) vector can be computed accordingly when preparing for the saccade initiation. In this example, the predicted saccade landing site (grey cross) will fall short of the target. Bottom: Upon saccade initiation, the stimulus will disappear and reappear to the left or right of the pre-saccadic location. If participant can use CD to remap the pre-saccadic location correctly, then vector *a* should match the actual stimulus displacement. Here in this example, the post-saccadic location is to the left of the pre-saccadic location, so the participant should judge the displacement as backward. However, if participant does not have access to complete CD information, saccade landing site may be used as a proxy of the pre-saccadic location. In this case, participant will perceive vector *b* as the target displacement and give a forward response instead (Rösler et al., 2015).

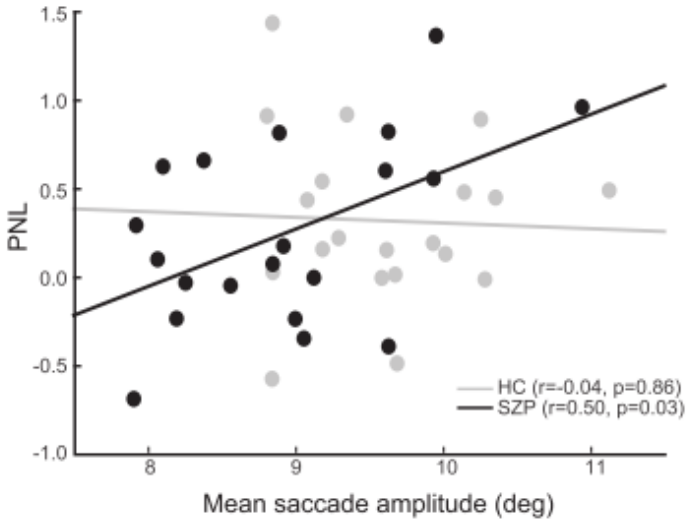

Figure 3. Blanking task performance in chronic SZP and HC. Mean saccade amplitude was correlated with judgment on pre-saccadic location of the stimulus in SZP, but not in HC (Rösler et al., 2015).

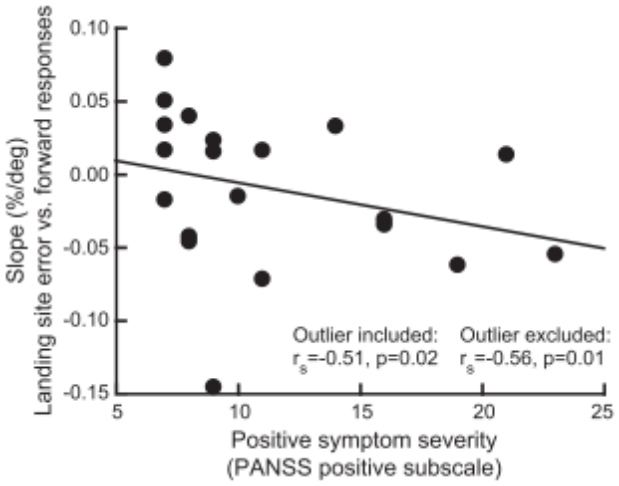

Figure 4. Blanking task performance and symptom severity in chronic SZP. When making perceptual judgments of target displacement, SZP with more severe positive symptom showed greater reliance on actual saccade landing site, consistent with less influence of CD signals (Rösler et al., 2015).

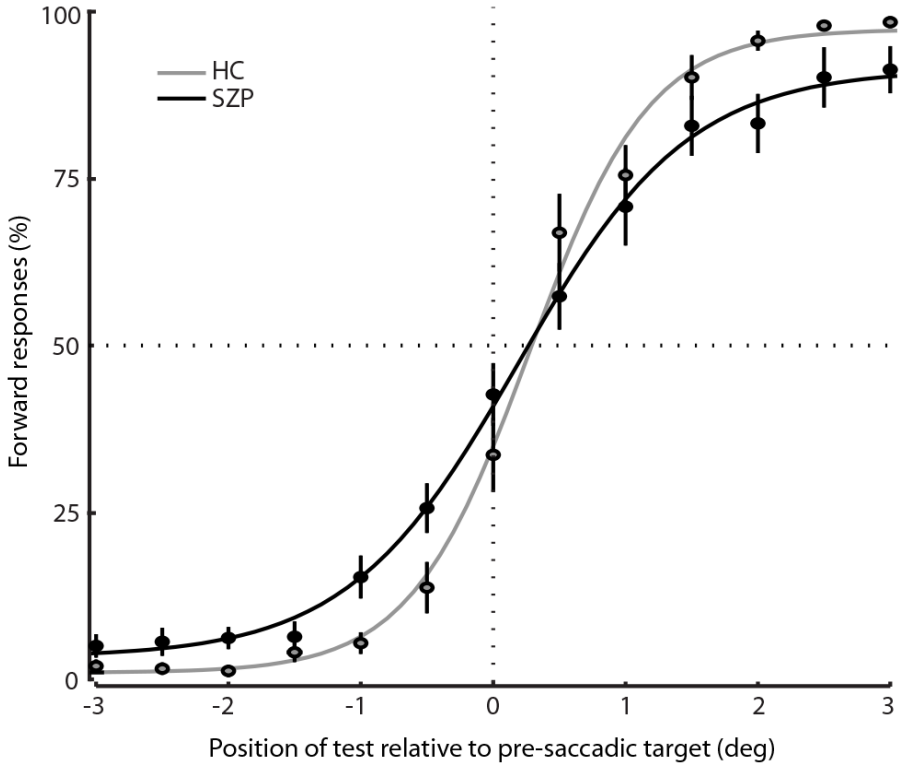

Figure 5. Group-averaged blanking task performance in chronic SZP and HC. Mean percentage of forward responses averaged over each group as a function of target displacement. On the x-axis, negative values mean backward jumps (towards the fixation) and positive values mean forward jumps (away from the fixation) relative to the pre-saccadic location (Rösler et al., 2015).

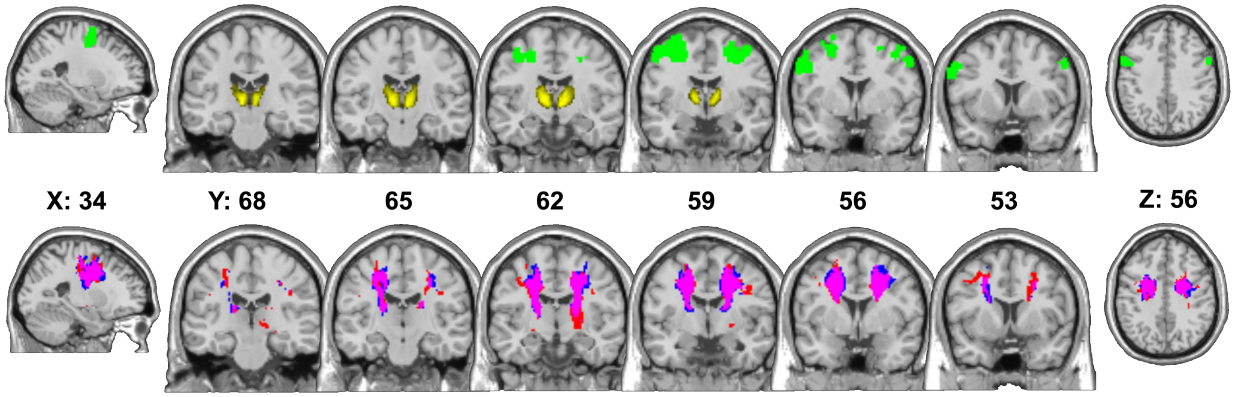

Figure 6. Probabilistic tractography results of the MDT-FEF pathway in both groups. Top panel: ROI masks projected onto a standard-space brain in multi-slice coronal view; bottom panel: group-averaged and thresholded white matter tracts in standard space. ROIs are color-coded as follows: FEF – green, MDT – yellow. Group tracts are color-coded as follows: HC tracts – red, SZP tracts – blue, overlapping areas – pink. Coordinates of each slice in standard space were presented in the middle.

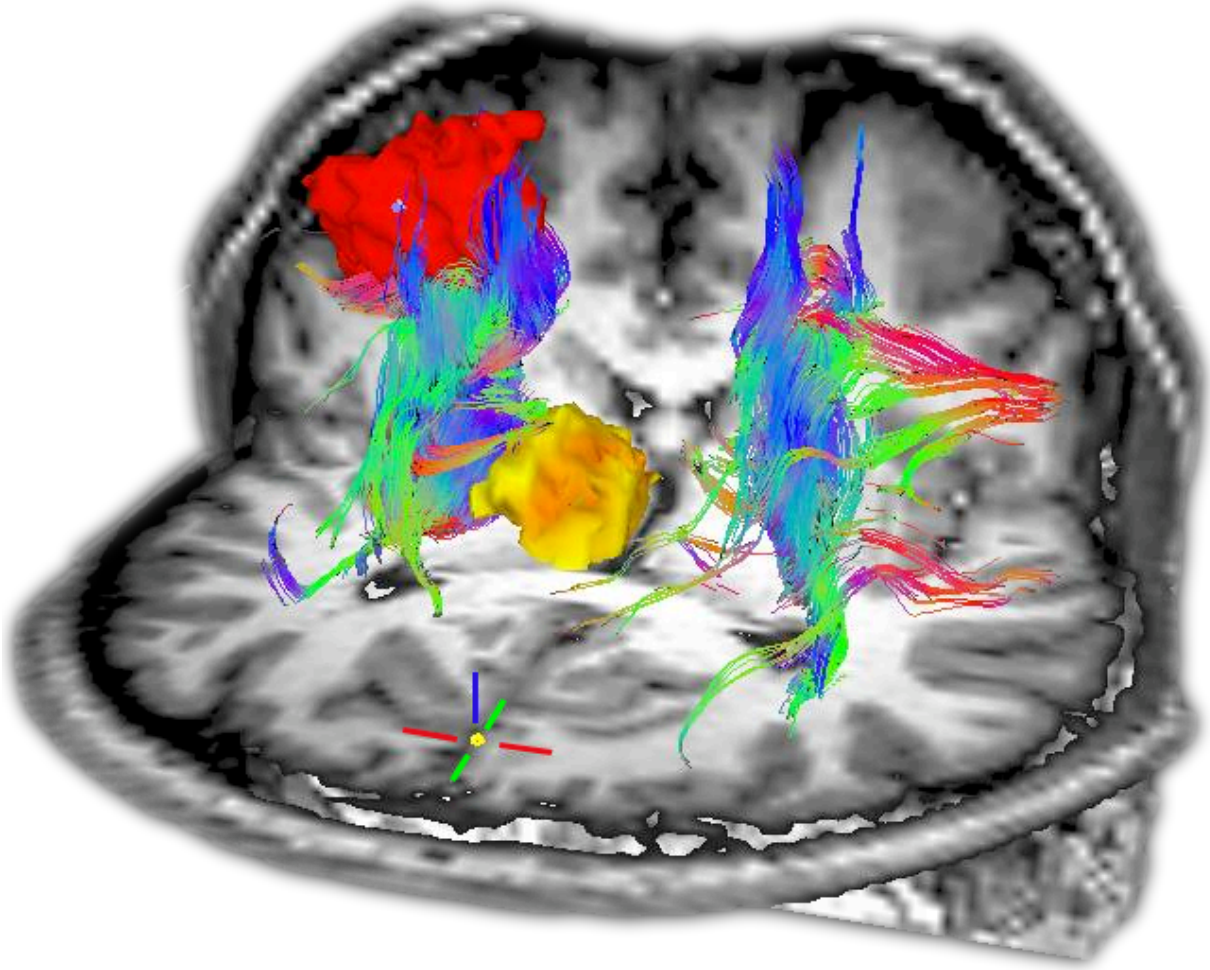

Figure 7. 3D Probabilistic tractography results of the MDT-FEF pathway in HC. 3D-rendered representations of the group-averaged and thresholded white matter tracts reverse normalized and overlaid on an HC participant's white matter skeleton, then projected onto the same participant's structural image using AFNI FATCAT Visualization. Results are essentially indistinguishable in SZP. ROIs are color-coded as follows: FEF – red; MDT – yellow. Fiber tract reconstructions are colored according to the DTI visualization convention (blue: superior-inferior, green: anterior-posterior, red: left-right).

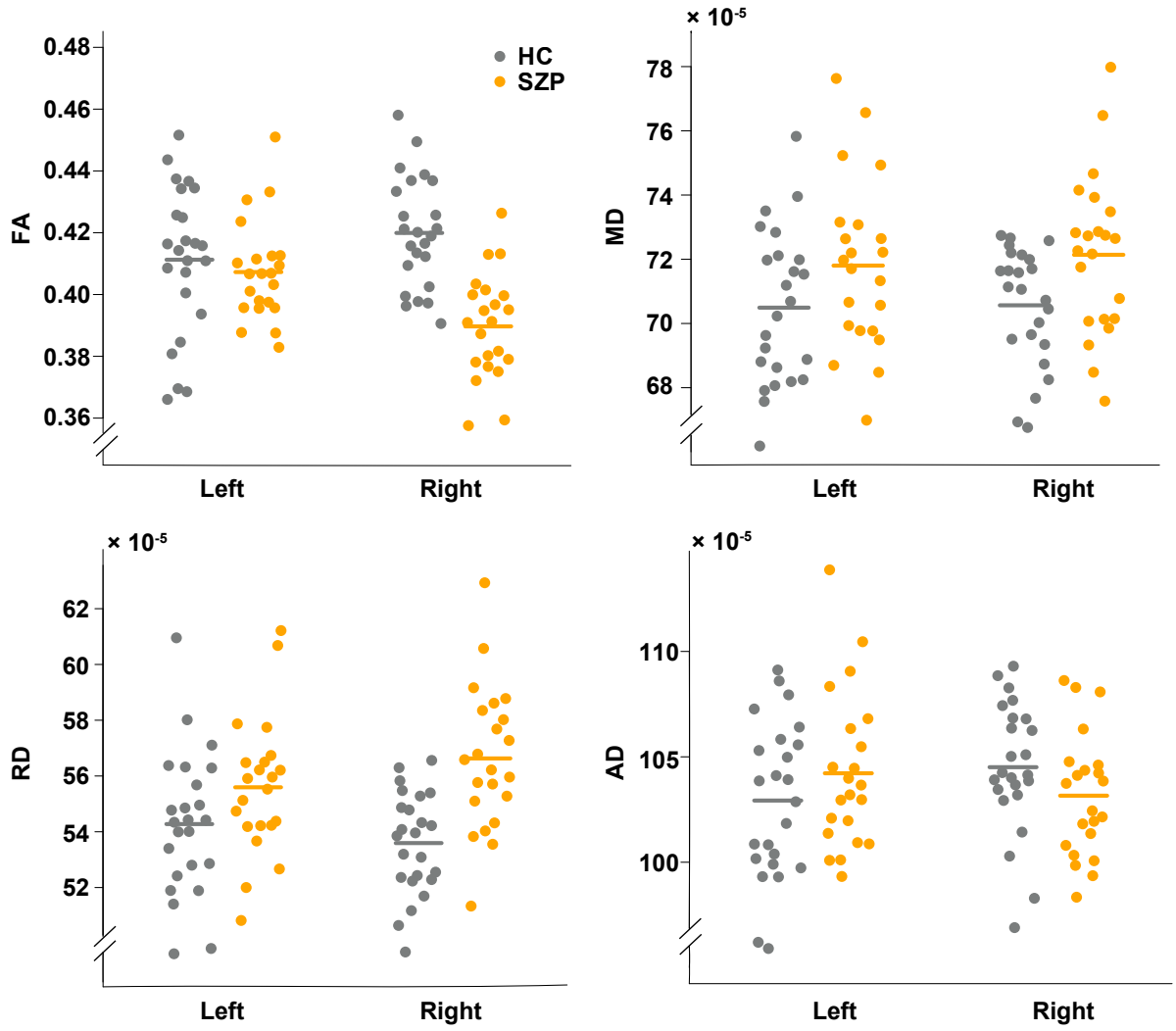

Figure 8. Group differences in the MDT-FEF tract microstructural integrity by hemisphere. Top left: FA; top right: MD; bottom left: RD; bottom right AD. AD: axial diffusivity; FA, fractional anisotropy; FEF, frontal eye fields; HC, healthy controls; MD, mean diffusivity; MDT, mediodorsal thalamus; RD, radial diffusivity; SZP, schizophrenia patients.

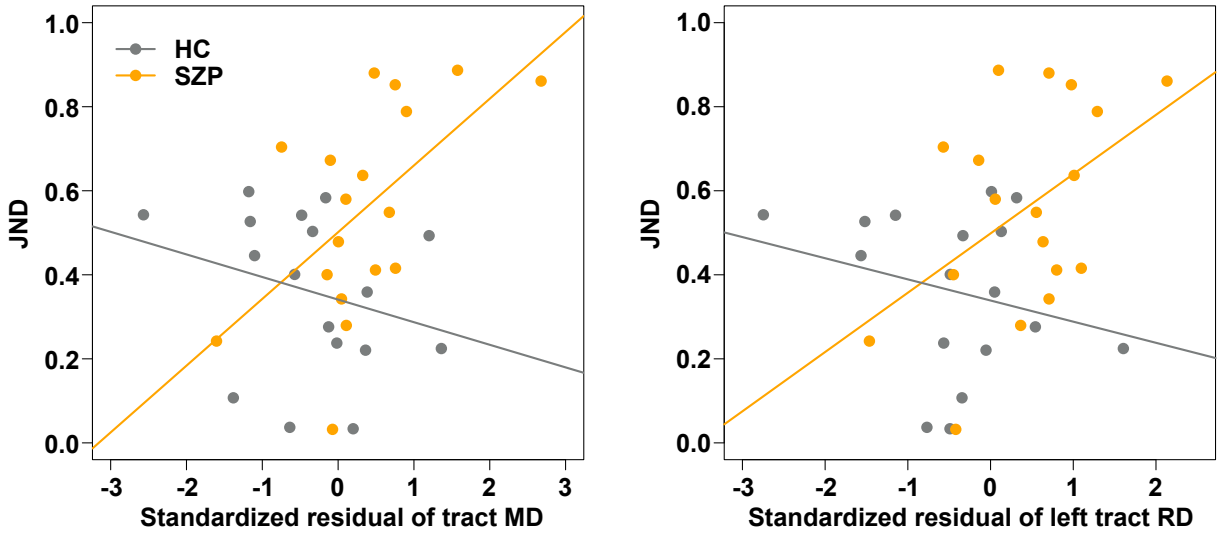

Figure 9. Scatterplots of JND against MDT-FEF tract-specific indices of microstructural integrity. Left: standardized residuals of MD across hemispheres; right: standardized residuals of RD of the left tract. These standardized values are 0 when equal to the whole brain MD or RD average, higher for more diffusive voxels and lower for less diffusive voxels. Smaller JND indicates more intact oculomotor CD signals. More compromised oculomotor CD signals correlated with more impaired white matter microstructure in SZP only. HC, healthy controls; JND, just noticeable difference; MD, mean diffusivity; RD, radial diffusivity; SZP, schizophrenia patients.

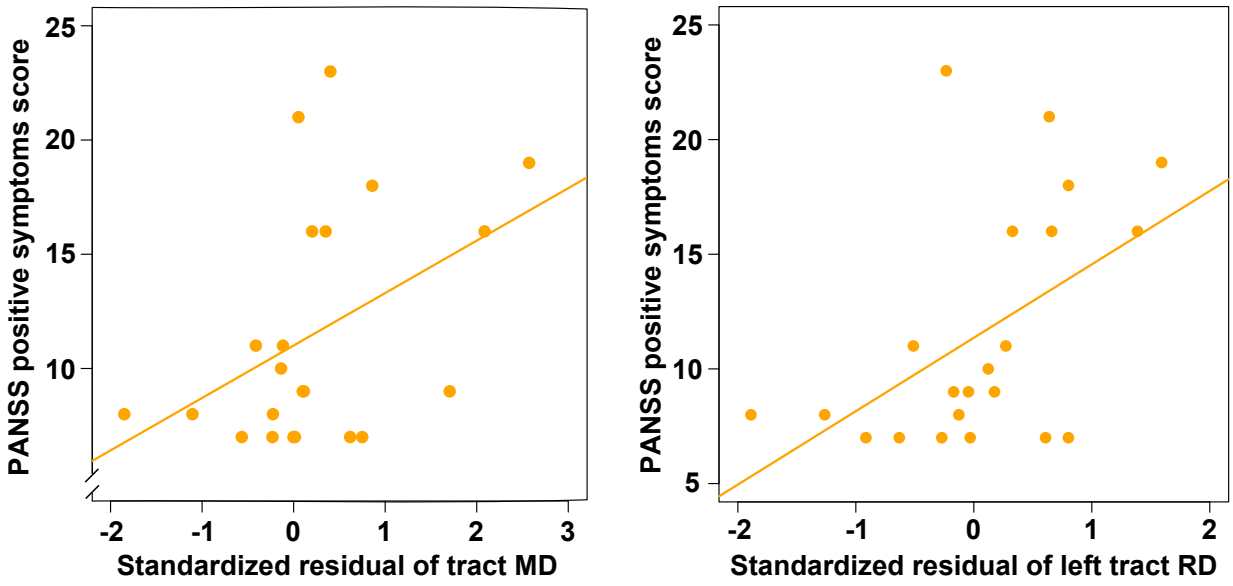

Figure 10. Scatterplots of PANSS positive symptoms scores against MDT-FEF tract-specific indices of microstructural integrity. Left: standardized residuals of MD across hemispheres; right: standardized residuals of RD of the left tract. These standardized values are 0 when equal to the whole brain MD or RD average, higher for more diffusive voxels and lower for less diffusive voxels. Larger PANSS scores indicate more severe symptoms. More severe positive symptoms correlated with more impaired white matter microstructure. MD, mean diffusivity; PANSS, Positive and Negative Syndrome Scale; RD, radial diffusivity.

APPENDIX C: Supplementary Results

Using the smaller subsample with behavioral data (see Table S1 for demographic information), the spatially normalized, group-averaged, and statistically thresholded MDT-FEF probabilistic tracts were very similar to those shown in Figure 6 and Figure 7. We performed a between-group t-test on whole brain probability values at each voxel. Again, no significant differences were found between the SZP and HC at the family-wise error rate of 0.05, indicating that the MDT-FEF pathway occupied the same spatial location in the brain.

Next, we conducted four repeated measures ANOVAs where one of the microstructural integrity measures (FA, MD, RD, AD) was the dependent variable each time, using diagnostic group as a between-subjects variable and hemisphere as a within-subject variable. Means and standard deviations are presented in Table S2. Again, higher microstructural integrity is indicated by higher FA values and lower MD, RD, and AD values. For FA, MD, and RD, there was a significant effect of group such that SZP showed evidence of reduced microstructural integrity of the MDT-FEF pathway (FA: $F(1,33) = 23.03$, $p < 0.001$, partial $\eta^2 = 0.41$; MD: $F(1,33) = 6.61$, $p = 0.015$, partial $\eta^2 = 0.17$; RD: $F(1,33) = 19.61$, $p < 0.001$, partial $\eta^2 = 0.37$). There was no group difference in tract AD, $F(1,33) = 0.34$, $p = 0.57$, partial $\eta^2 = 0.01$. For FA and RD, there was an additional hemisphere effect such that the MDT-FEF pathway in the right hemisphere showed lower microstructural integrity than that in the left hemisphere across groups (FA: $F(1,33) = 9.56$, $p = 0.004$, partial $\eta^2 = 0.23$; RD: $F(1,33) = 4.26$, $p = 0.047$, partial $\eta^2 = 0.11$). This hemisphere effect was not significant for MD, $F(1,33) = 2.98$, $p = 0.09$, partial $\eta^2 = 0.08$. For FA only, there was a group × hemisphere interaction effect, $F(1, 33) = 7.97$, $p = 0.008$, partial $\eta^2 = 0.19$, such that the hemisphere effect was only significant in SZP, $t(17) = 4.01$, $p = 0.001$, but not in HC, $t(16) = 0.20$, $p = 0.84$. This group × hemisphere interaction effect was not

significant for MD or RD (MD: $F(1,33) = 0.00$, $p = 1.0$, partial $\eta^2 = 0.00$; RD: $F(1,33) = 3.58$, $p = 0.07$, partial $\eta^2 = 0.10$). There were no correlations between CPZ equivalent dose and any of the microstructural integrity measures ($-0.49 < r_s < 0.15$, $0.06 < p < 0.77$).

Table S1. Demographic information of the subset sample with behavioral data

	HC (n = 17)	SZP (n = 18)		
	Mean (SD)	Mean (SD)	Statistic	p
Age (Years)	34.1 (8.9)	36.7 (8.2)	t = -0.9	0.37
Sex (Female/Male)	7/10	2/16	χ^2 = 4.1	0.06
IQ[a]	99.2 (14.6)	95.8 (12.2)	t = 0.7	0.48
Education[b]	7.2 (1.1)	4.9 (1.8)	t = 4.6	< .001
Handedness[c]	0.85 (0.49)	0.93 (0.20)	t = -0.7	0.49
Illness Duration (Years)		14.6 (5.4)		
PANSS Positive		11.4 (5.2)		
PANSS Negative		12.6 (6.1)		
PANSS General		24.6 (7.9)		
CPZ Equivalent (mg)		302.0 (257.7)		

Notes: CPZ, chlorpromazine; HC, healthy control subjects; PANSS, Positive and Negative Syndrome Scale; SZP, patients with schizophrenia.
[a]Based on the Nederlandse Leestest voor Volwassenen.
[b]Education category: 0 = <6 years of primary education; 1 = finished 6 years of primary education; 2 = 6 years of primary education and low-level secondary education; 3 = 4 years of low-level secondary education; 4 = 4 years of average-level secondary education; 5 = 5 years of average-level secondary education; 6 = 4 years of secondary vocational training; 7 = 4 years of high-level professional education; 8 = university degree.
[c]Based on the Edinburgh Handedness Inventory; scores range from 0 indicating complete left-handedness to 1 indicating complete right-handedness.

Table S2. Mean microstructural integrity measures (FA, MD, RD, AD) in the MDT-FEF tract by hemisphere in the subset sample with behavioral data.

		HC (n = 17)	SZP (n = 18)
		Mean (SD)	Mean (SD)
FA	Left	0.43 (0.02)	0.41 (0.02)
	Right	0.43 (0.02)	0.39 (0.02)
MD	Left	6.98×10^{-4} (2.15×10^{-5})	7.16×10^{-4} (2.42×10^{-5})
	Right	7.01×10^{-4} (1.92×10^{-5})	7.20×10^{-4} (2.30×10^{-5})
RD	Left	5.27×10^{-4} (2.22×10^{-5})	5.54×10^{-4} (2.24×10^{-5})
	Right	5.28×10^{-4} (1.87×10^{-5})	5.63×10^{-4} (2.31×10^{-5})
AD	Left	1.04×10^{-3} (3.65×10^{-5})	1.04×10^{-3} (3.50×10^{-5})
	Right	1.05×10^{-3} (3.31×10^{-5})	1.03×10^{-3} (2.95×10^{-5})

Notes: AD: axial diffusivity; FA, fractional anisotropy; FEF, frontal eye fields; HC, healthy controls; MD, mean diffusivity; MDT, mediodorsal thalamus; RD, radial diffusivity; SZP, schizophrenia patients.

REFERENCES

REFERENCES

Abe, O., Aoki, S., Hayashi, N., Yamada, H., Kunimatsu, A., Mori, H., … Ohtomo, K. (2002). Normal aging in the central nervous system: Quantitative MR diffusion-tensor analysis. *Neurobiology of Aging, 23(3),* 433–441.

Alexander, A. L., Lee, J. E., Lazar, M., & Field, A. S. (2007). Diffusion tensor imaging of the brain. *Neurotherapeutics, 4(3),* 316–329.

Andersson, J. L. R., & Skare, S. (2002). A model-based method for retrospective correction of geometric distortions in diffusion-weighted EPI. *NeuroImage, 16(1),* 177–199.

Andreasen, N. C. (1999). A unitary model of schizophrenia. *Archives of General Psychiatry, 56(9),* 781–787.

Andreasen, N. C., Flaum, M., & Arndt, S. (1992). The Comprehensive Assessment of Symptoms and History (CASH). An instrument for assessing diagnosis and psychopathology. *Archives of General Psychiatry, 49(8),* 615–623.

Anticevic, A., Cole, M. W., Repovs, G., Murray, J. D., Brumbaugh, M. S., Winkler, A. M., … Glahn, D. C. (2014). Characterizing thalamo-cortical disturbances in schizophrenia and bipolar illness. *Cerebral Cortex, 24(12),* 3116–3130.

Anticevic, A., Haut, K., Murray, J. D., Repovs, G., Yang, G. J., Diehl, C., … Cannon, T. D. (2015). Association of thalamic dysconnectivity and conversion to psychosis in youth and young adults at elevated clinical risk. *JAMA Psychiatry, 72(9),* 882–891.

Anticevic, A., Yang, G., Savic, A., Murray, J. D., Cole, M. W., Repovs, G., … Glahn, D. C. (2014). Mediodorsal and visual thalamic connectivity differ in schizophrenia and bipolar disorder with and without psychosis history. *Schizophrenia Bulletin, 40(6),* 1227–1243.

Ashburner, J., & Friston, K. J. (2005). Unified segmentation. *NeuroImage, 26(3),* 839–851.

Behrens, T. E. J., Berg, H. J., Jbabdi, S., Rushworth, M. F. S., & Woolrich, M. W. (2007). Probabilistic diffusion tractography with multiple fibre orientations: What can we gain? *NeuroImage, 34(1),* 144–155.

Behrens, T. E. J., Woolrich, M. W., Jenkinson, M., Johansen-Berg, H., Nunes, R. G., Clare, S., … Smith, S. M. (2003). Characterization and propagation of uncertainty in diffusion-weighted MR imaging. *Magnetic Resonance in Medicine, 50(5),* 1077–1088.

Blakemore, S.-J., Smith, J., Steel, R., Johnstone, E. C., & Frith, C. D. (2000). The perception of self-produced sensory stimuli in patients with auditory hallucinations and passivity experiences: evidence for a breakdown in self-monitoring. *Psychological Medicine, 30(5),*

1131–1139.

Canu, E., Agosta, F., & Filippi, M. (2015). A selective review of structural connectivity abnormalities of schizophrenic patients at different stages of the disease. *Schizophrenia Research, 161(1),* 19–28.

Carrera, E., & Bogousslavsky, J. (2006). The thalamus and behavior: Effects of anatomically distinct strokes. *Neurology, 66(12),* 1817–1823.

Cavanagh, P., Hunt, A. R., Afraz, A., & Rolfs, M. (2010). Visual stability based on remapping of attention pointers. *Trends in Cognitive Sciences, 14(4),* 147–153.

Cavanaugh, J., Berman, R. A., Joiner, W. M., & Wurtz, R. H. (2016). Saccadic corollary discharge underlies stable visual perception. *Journal of Neuroscience, 36(1),* 31–42.

Collins, T., Rolfs, M., Deubel, H., & Cavanagh, P. (2009). Post-saccadic location judgments reveal remapping of saccade targets to non-foveal locations. *Journal of Vision, 9(5),* 1–9.

Corlett, P. R., Honey, G. D., & Fletcher, P. C. (2016). Prediction error, ketamine and psychosis: An updated model. *Journal of Psychopharmacology, 30(11),* 1–11.

Crail-Melendez, D., Atriano-Mendieta, C., Carrillo-Meza, R., & Ramirez-Bermudez, J. (2013). Schizophrenia-like psychosis associated with right lacunar thalamic infarct. *Neurocase, 19(1),* 22–26.

Cropley, V. L., Klauser, P., Lenroot, R. K., Bruggemann, J., Sundram, S., Bousman, C., … Zalesky, A. (2017). Accelerated gray and white matter deterioration with age in schizophrenia. *American Journal of Psychiatry, 174(3),* 286–295.

Davis, K. L., Stewart, D. G., Friedman, J. I., Buchsbaum, M., Harvey, P. D., Hof, P. R., … Haroutunian, V. (2003). White matter changes in schizophrenia. *Archives of General Psychiatry, 60(5),* 443-456.

Desikan, R. S., Ségonne, F., Fischl, B., Quinn, B. T., Dickerson, B. C., Blacker, D., … Killiany, R. J. (2006). An automated labeling system for subdividing the human cerebral cortex on MRI scans into gyral based regions of interest. *NeuroImage, 31(3),* 968–980.

Deubel, H., Schneider, W. X., & Bridgeman, B. (1996). Postsaccadic target blanking prevents saccadic suppression of image displacement. *Vision Research, 36(7),* 985–996.

Feinberg, I. (1978). Efference copy and corollary discharge: implications for thinking and its disorders. *Schizophrenia Bulletin, 4(4),* 636–640.

Feinberg, I., & Guazzelli, M. (1999). Schizophrenia--a disorder of the corollary discharge systems that integrate the motor systems of thought with the sensory systems of consciousness. *The British Journal of Psychiatry, 174(3),* 196–204.

Fletcher, P. C., & Frith, C. D. (2009). Perceiving is believing: a Bayesian approach to explaining the positive symptoms of schizophrenia. Nature Reviews. *Neuroscience, 10(1),* 48–58.

Ford, J. M., & Mathalon, D. H. (2012). Anticipating the future: Automatic prediction failures in schizophrenia. *International Journal of Psychophysiology, 83(2),* 232–239.

Ford, J. M., Mathalon, D. H., Roach, B. J., Keedy, S. K., Reilly, J. L., Gershon, E. S., & Sweeney, J. A. (2013). Neurophysiological evidence of corollary discharge function during vocalization in psychotic patients and their nonpsychotic first-degree relatives. *Schizophrenia Bulletin, 39(6),* 1272–1280.

Gaymard, B., Rivaud, S., & Pierrot-Deseilligny, C. (1994). Impairment of extraretinal eye position signals after central thalamic lesions in humans. *Experimental Brain Research, 102,* 1–9.

Genetic Risk and Outcome in Psychosis (GROUP) Investigators. (2011). Evidence that familial liability for psychosis is expressed as differential sensitivity to cannabis: an analysis of patient-sibling and sibling-control pairs. *Archives of General Psychiatry, 68(2),* 138–147.

Giraldo-Chica, M., Rogers, B. P., Damon, S. M., Landman, B. A., & Woodward, N. D. (2018). Prefrontal-thalamic anatomical connectivity and executive cognitive function in schizophrenia. *Biological Psychiatry, 83(6),* 509–517.

Gray, J. A., Feldon, J., Rawlins, J. N. P., Hemsley, D. R., & Smith, A. D. (1991). The neuropsychology of schizophrenia. *Behavioral and Brain Sciences, 14(1),* 1–20.

Green, M. F., & Kinsbourne, M. (1990). Subvocal activity and auditory hallucinations: clues for behavioral treatments? *Schizophrenia Bulletin, 16(4),* 617–625.

Hallett, P. E., & Lightstone, A. D. (1976a). Saccadic eye movements to flashed targets. *Vision Research, 16(1),* 107–114.

Hallett, P. E., & Lightstone, A. D. (1976b). Saccadic eye movements towards stimuli triggered by prior saccades. *Vision Research, 16(1),* 99–106.

Islam, F., Mulsant, B. H., Voineskos, A. N., & Rajji, T. K. (2017). Brain-derived neurotrophic factor expression in individuals with schizophrenia and healthy aging: Testing the accelerated aging hypothesis of schizophrenia. *Current Psychiatry Reports, 19(7),* 36.

Kay, S. R., Fiszbein, A., & Opler, L. A. (1987). The Positive and Negative Syndrome Scale (PANSS) for schizophrenia. *Schizophrenia Bulletin, 13(2),* 261–276.

Landman, B. A., Bogovic, J. A., Wan, H., ElShahaby, F. E. Z., Bazin, P.-L., & Prince, J. L. (2012). Resolution of crossing fibers with constrained compressed sensing using diffusion tensor MRI. *NeuroImage, 59(3),* 2175–2186.

Lee, J., & Park, S. (2005). Working memory impairments in schizophrenia: A meta-analysis. *Journal of Abnormal Psychology, 114(4),* 599–611.

Mori, S., & van Zijl, P. C. M. (2002). Fiber tracking: principles and strategies - a technical review. *NMR in Biomedicine, 15(7–8),* 468–480.

Mori, S., & Zhang, J. (2006). Principles of diffusion tensor imaging and its applications to basic neuroscience research. *Neuron, 51(5),* 527–539.

Neggers, S. F. W., Zandbelt, B. B., Schall, M. S., & Schall, J. D. (2015). Comparative diffusion tractography of corticostriatal motor pathways reveals differences between humans and macaques. *Journal of Neurophysiology, 113(7),* 2164–2172.

Ostendorf, F., Liebermann, D., & Ploner, C. J. (2010). Human thalamus contributes to perceptual stability across eye movements. *Proceedings of the National Academy of Sciences, 107(3),* 1229–1234.

Pergola, G., Selvaggi, P., Trizio, S., Bertolino, A., & Blasi, G. (2015). The role of the thalamus in schizophrenia from a neuroimaging perspective. *Neuroscience & Biobehavioral Reviews, 54,* 57–75.

Ramsay, I. S., & MacDonald, A. W. (2018). The ups and downs of thalamocortical connectivity in schizophrenia. *Biological Psychiatry, 83(6),* 473–474.

Rösler, L., Rolfs, M., van der Stigchel, S., Neggers, S. F. W., Cahn, W., Kahn, R. S., & Thakkar, K. N. (2015). Failure to use corollary discharge to remap visual target locations is associated with psychotic symptom severity in schizophrenia. *Journal of Neurophysiology, 114(2),* 1129–1136.

Schneider, K. (1959). *Clinical Psychopathology.* New York, NY: Grune &Stratton.

Shepherd, A. M., Laurens, K. R., Matheson, S. L., Carr, V. J., & Green, M. J. (2012). Systematic meta-review and quality assessment of the structural brain alterations in schizophrenia. *Neuroscience & Biobehavioral Reviews, 36(4),* 1342–1356.

Shergill, S. S., Samson, G., Bays, P. M., Frith, C. D., & Wolpert, D. M. (2005). Evidence for sensory prediction deficits in schizophrenia. *American Journal of Psychiatry, 162(12),* 2384–2386.

Sherman, S. M. (2016). Thalamus plays a central role in ongoing cortical functioning. *Nature Neuroscience, 19(4),* 533–541.

Sim, K., Yang, G. L., Loh, D., Poon, L. Y., Sitoh, Y. Y., Verma, S., … Pantelis, C. (2009). White matter abnormalities and neurocognitive deficits associated with the passivity phenomenon in schizophrenia: A diffusion tensor imaging study. *Psychiatry Research - Neuroimaging, 172(2),* 121–127.

Smith, S. M., Jenkinson, M., Woolrich, M. W., Beckmann, C. F., Behrens, T. E. J., Johansen-Berg, H., … Matthews, P. M. (2004). Advances in functional and structural MR image analysis and implementation as FSL. *NeuroImage, 23(SUPPL. 1),* S208–S219.

Snook, L., Plewes, C., & Beaulieu, C. (2007). Voxel based versus region of interest analysis in diffusion tensor imaging of neurodevelopment. *NeuroImage, 34(1),* 243–252.

Sommer, M. A., & Wurtz, R. H. (2002). A pathway in primate brain for internal monitoring of movements. *Science, 296(5572),* 1480–1482.

Sommer, M. A., & Wurtz, R. H. (2004). What the brain stem tells the frontal cortex. II. Role of the SC-MD-FEF pathway in corollary discharge. *Journal of Neurophysiology, 91(3),* 1403–1423.

Sommer, M. A., & Wurtz, R. H. (2008). Brain circuits for the internal monitoring of movements. *Annual Review of Neuroscience, 31,* 317–338.

Song, S.-K., Sun, S.-W., Ramsbottom, M. J., Chang, C., Russell, J., & Cross, A. H. (2002). Dysmyelination revealed through MRI as increased radial (but unchanged axial) diffusion of water. *NeuroImage, 17(3),* 1429–1436.

Thakkar, K. N., Diwadkar, V. A., & Rolfs, M. (2017). Oculomotor prediction: A window into the psychotic mind. *Trends in Cognitive Sciences, 21(5),* 344–356.

Thakkar, K. N., van den Heiligenberg, F. M. Z., Kahn, R. S., & Neggers, S. F. W. (2014). Frontal-subcortical circuits involved in reactive control and monitoring of gaze. *Journal of Neuroscience, 34(26),* 8918–8929.

Welsh, R. C., Chen, A. C., & Taylor, S. F. (2010). Low-frequency BOLD fluctuations demonstrate altered thalamocortical connectivity in schizophrenia. *Schizophrenia Bulletin, 36(4),* 713–722.

Wing, J. K., Babor, T., Brugha, T., Burke, J., Cooper, J. E., Giel, R., … Sartorius, N. (1990). SCAN: Schedules for Clinical Assessment in Neuropsychiatry. *Archives of General Psychiatry, 47(6),* 589–593.

Woods, S. W. (2003). Chlorpromazine equivalent doses for the newer atypical antipsychotics. *The Journal of Clinical Psychiatry, 64(6),* 663–667.

Woodward, N. D., Karbasforoushan, H., & Heckers, S. (2012). Thalamocortical dysconnectivity in schizophrenia. *American Journal of Psychiatry, 169(10),* 1092–1099.

Yoon, J. H., Sheremata, S. L., Rokem, A., & Silver, M. A. (2013). Windows to the soul: vision science as a tool for studying biological mechanisms of information processing deficits in schizophrenia. *Frontiers in Psychology, 4*, 681.

Zhou, Y., Fox, D., Anand, A., Elhaj, A., Kapoor, A., Najibi, F., … Jayam-Trouth, A. (2015). Artery of percheron infarction as an unusual cause of Korsakoff's syndrome. *Case Reports in Neurological Medicine, 2015,* 1–6.